
Article:
Flintoft, I D orcid.org/0000-0003-3153-8447, Robinson, M P orcid.org/0000-0003-1767-5541, Melia, G C R et al. (2 more authors) (2014) Average absorption cross-section of the human body measured at 1-12 GHz in a reverberant chamber:results of a human volunteer study. Physics in Medicine and Biology. pp. 3297-3317. ISSN: 0031-9155

https://doi.org/10.1088/0031-9155/59/13/3297

Average absorption cross-section of the human body measured at 1-12 GHz in a reverberant environment: Results of a human volunteer study

I. D. Flintoft[1], M. P. Robinson[1], G. C. R. Melia[2], J. F. Dawson[1] and A. C. Marvin[1]

[1] *Department of Electronics, University of York, Heslington, York YO10 5DD, UK*
[2] *Medical Physics Department, Freeman Hospital, Newcastle upon Tyne NE7 7DN, UK*

Physics in Medicine and Biology, vol. 59, no. 13, pp. 3297-3317, 2014

Accepted for publication 06/05/2014

Statement of Provenance

Average Absorption Cross-Section of the Human Body Measured at 1-12 GHz in a Reverberant Chamber: Results of a human volunteer study

I. D. Flintoft, M. P. Robinson, G. C. R. Melia, A. C. Marvin, J. F. Dawson

Department of Electronics, University of York, Heslington, York YO10 5DD, UK
Corresponding author's email: ian.flintoft@york.ac.uk

Submitted to Physics in Medicine and Biology, 27th January 2014

Abstract

The electromagnetic absorption cross-section (ACS) averaged over polarisation and angle-of-incidence of 60 ungrounded adult subjects was measured at microwave frequencies of 1-12 GHz in a reverberation chamber. Average ACS is important in non-ionising dosimetry and exposure studies, and is closely related to the whole-body averaged specific absorption rate (WBSAR). The average ACS was measured with a statistical uncertainty of less than 3 % and high frequency resolution for individuals with a range of body shapes and sizes allowing the statistical distribution of WBSAR over a real population with individual internal and external morphologies to be determined. The average ACS of all subjects was found to vary from 0.15 to 0.4 m^2; for an individual subject it falls with frequency over 1-6 GHz, and then rises slowly over 6-12 GHz range in which few other studies have been conducted. Average ACS and WBSAR are then used as a surrogate for worst-case ACS/WBSAR in order to study their variability across a real population compared to literature results from simulations using numerical phantoms with a limited range of anatomies. Correlations with body morphological parameters such as height, mass and waist circumference have been investigated: the strongest correlation is with body surface area (BSA) at all frequencies above 1 GHz, however direct proportionality to BSA is not established until above 5 GHz. When average ACS is normalised to BSA, the resulting absorption efficiency shows a negative correlation with the estimated thickness of subcutaneous body fat. Surrogate models and statistical analysis of the measurement data are presented and compared to similar models from the literature. The overall dispersion of measured average WBSAR of the sample of the UK population studied is consistent with the dispersion of simulated worst-case WBSAR across multiple numerical phantom families. The statistical results allow the calibration of human exposure assessments made with particular phantoms to a population with individual morphologies.

PACS codes: 41.20.Jb, 87.19.rf, 87.50.sj

1. Introduction

The absorption cross-section (ACS) describes how much power a plane electromagnetic (EM) wave deposits in the human body. It is closely related to the whole-body averaged specific absorption rate (WBSAR), which is one of the most important parameters in international guidelines that limit exposure to non-ionising radiation (ICNIRP 1998). ICNIRP adopts a basic restriction of 0.08 W/kg on WBSAR in the frequency range 10 MHz to 10 GHz for public exposure in order to avoid adverse health effects due to heating. Above 10 GHz, where the interaction is confined to the body surface, the external power density is taken as the basic restriction and the associated limit is 10 W m^{-2}. For a given subject, ACS and WBSAR vary with frequency and the direction and polarisation of the incident wave. Most studies consider

the worst-case geometry for the angle of incidence and polarisation since this is the salient case for exposure assessment and compliance with the basic restrictions in the guidelines; typically for WBSAR this is a vertically polarised electric field incident from the front of the body with its wave vector parallel to the ground. ACS and WBSAR can be estimated using analytical methods at low frequencies and with geometric optics approximations in the high frequency limit, using simplifying assumptions about body shape and internal anatomy. These assumptions are usually made in such a way that the predictions are conservative with respect to the worst case exposure. The geometric optics (GO) regime, in which more efficient asymptotic computational methods can be applied, is not fully established for whole body exposure until at least 10 GHz, as demonstrated by our results.

In recent years numerical techniques, such as finite-difference time-domain (FDTD), have been widely applied to the calculation of WBSAR and the assessment of compliance with the safety guidelines in particular exposure scenarios: A recent review is given by Hand (2008). One of the primary aims of such studies is to determine if the external reference levels are conservative with regard to the basic restriction on SAR in particular scenarios or in cases where reference levels are exceeded to establish compliance with the basic restriction and derive bespoke guidelines for the specific scenario. This approach can yield accurate results, but for a limited range of numerical phantoms and electrical parameters for the tissues (Dimbylow *et al* 2008). Such approaches require considerable computational effort, especially at higher frequencies which necessitate a finer numerical discretisation, and new phantoms with different anatomies are expensive to develop as noted by Hirata *et al* (2008). Numerical phantoms are also difficult to transform into different body postures while maintaining the correct internal anatomies (Findlay and Dimbylow 2005, Nagaoka and Watanabe 2008). Most studies have been limited to considering a few angles of incidence and polarisations, typically the worst-case for WBSAR exposure, though more recent studies have varied the direction of incidence (Uusitupa *et al* 2010, Conil *et al* 2011, Wang *et al* 2012).

Phantom internal morphology has been found to be an important factor in the determination of WBSAR (Dimbylow *et al* 2008, Conil *et al* 2008). El Habachi *et al* (2010) conclude that internal morphological parameters are equally important as external parameters for building surrogate models for WBSAR applicable to whole populations and that obtaining the statistical distribution of WBSAR for a given population is therefore very difficult; they therefore propose an approach based on randomised internal morphology. El Habachi *et al* (2010) also point out that numerical phantoms have not been chosen according to experimental design methods and therefore there is a need to test the results predicted by phantom simulations against real populations in order to assess the validity of surrogate models determined from the limited range of phantoms available. This is particularly the case for families of phantoms where scaling is employed and a diverse range of internal anatomies may not be sampled (Dimbylow *et al* 2008). Hence there is a motivation to develop a measurement-based approach in the frequency band up to 10 GHz to validate the predictions of simulations used in human exposure assessment and the surrogate models determined from them across real populations of subjects. A direct measurement approach also allows statistical information about individual exposure and morphology to be collected, which could be of use in epidemiological studies of environmental exposure of populations.

ACS and WBSAR are hard to measure in-situ with real subjects; however, reverberant environments provide an opportunity to accomplish this. The need to study non-ionising exposure in real environments, rather than unrealistic worst-case scenarios, has already led to increasing interest in reverberant environments (Neubauer *et al* 2009). Reverberant environments allow the average (over angle of incidence and polarisation) power absorbed by a subject to be measured directly and hence the correspondingly averaged ACS and WBSAR to be determined. Henceforth when we refer to “average” ACS or WBSAR it will be this average over directions and polarisations rather than a whole body average unless explicitly stated otherwise. The EM fields in such environments are expected to follow Rician statistics,

with a 'K-factor' that characterises the relative contributions of the direct and multiply-reflected waves, also called the 'diffuse multiple channels' and 'line of sight' paths (Bamba *et al* 2013). So far this approach has mainly been applied to in-situ estimation of average absorption (Andersen *et al* 2012, Bamba *et al* 2013). The only precise laboratory based average ACS measurement studies we are aware of are by Wang *et al* (2012) and Senic *et al* (2013). Wang et al. (2012) measured only three spot frequencies and a single volunteer and Senic *et al* (2013) considered a single grounded subject over a large range of 0.2-8 GHz. While such measurements do not allow the direct determination of worst-case WBSAR, corresponding to the particular direction and polarisation of wave that give the maximum absorbed power, it is still possible to use average ACS to quantify the variability of power absorption across a real population and to investigate its dependence on external morphological parameters. Statistical information on the dependence of ACS on internal morphological parameters can also be obtained.

In this paper we apply a metrological reverberation chamber to high accuracy controlled measurement of average ACS/WBSAR, thereby allowing many of the underlying assumptions and uncertainties of numerical approaches to WBSAR determination to be tested against a real population of subjects including varied body shapes, postures, internal anatomies and electrical parameters (which depend on age, body hydration and other physiological parameters). Our measurement technique, originally developed to investigate the effect of human bodies on radio propagation in aircraft (Melia *et al* 2013), has been optimised for fast high accuracy controlled laboratory measurement of ACS over a broad frequency range (Melia 2013). In previous work (Melia *et al* 2013) we measured the average ACS of 9 bodies with a total measurement uncertainty of over 10 % and long measurement time that led to large systematic uncertainties due to posture variation during the measurement. We have now investigated a much larger group of 60 subjects with our optimised methodology over the frequency range 1-12 GHz, which includes the intermediate frequency regime in which standing waves in the fat layer affect ACS most strongly. The lower frequency limit of 1 GHz is determined by the size of the measurement apparatus and could in principle be reduced, though other effects will ultimately restrict this to a few hundred megahertz. Our measurements were taken to frequencies above 10 GHz, the maximum frequency of the ICNIRP basic restriction on WBSAR, in order to allow the GO limit to become more fully established as an aid to validating the expected correlations of ACS with body surface area. Most reported studies of WBSAR are limited to frequencies below 3-6 GHz so the measurements above these frequencies provide new confirmation of the expected trends at the higher frequencies of the ICNIRP guidelines. The results are compared to other ACS and WBSAR studies. We have also investigated possible correlations between average ACS/WBSAR and easily measured body parameters such as mass and height, as well as indirectly estimated quantities including body surface area and subcutaneous fat thickness.

2. Absorption cross-section

2.1 Definition of ACS

The absorption cross-section of the body for a linearly polarised plane-wave with power density S^{i} incident from direction with spherical polar angles (θ, φ) is defined as

$$\sigma_p^{\mathrm{a}}(\theta, \varphi) = \frac{P^{\mathrm{a}}}{S^{\mathrm{i}}}, \tag{1}$$

where P^{a} is the total power absorbed in the body. Here p denotes the polarisation direction of the wave and the power density is the product of the root-mean-square electric and magnetic field amplitudes of the plane-wave. A related quantity is the whole-body specific absorption rate (WBSAR) which is the absorbed power divided by the mass of the body m:

$$WBSAR_p(\theta,\phi) = \frac{P^a}{m} = \frac{S^i}{m}\sigma^a_p(\theta,\phi)\ . \tag{2}$$

In a reverberant environment there are multiple reflections and many EM waves are incident on the body simultaneously from different directions and with different polarisations. The relevant parameter is then the ACS averaged over all polarisations and directions of incidence, $\langle \sigma^a \rangle$. In the case of an ideally reverberant environment, as closely approximated by a metrological reverberation chamber used in this study, statistically equal power density is incident from every direction and with each polarisation (Hill 2009). The average ACS is then given by

$$\langle \sigma^a \rangle = \frac{1}{8\pi} \oiint_{4\pi} \left(\sigma^a_{TE}(\theta,\phi) + \sigma^a_{TM}(\theta,\phi) \right) \mathrm{d}\Omega\ , \tag{3}$$

where the polarisation average is taken over two independent polarisation directions, transverse electric (TE) and transverse magnetic (TM), to the plane of incidence (Carlberg 2004).

2.3 Absorption efficiency and the geometric optics limit

In the GO limit, where the wavelength is much shorter than the radii of curvature of the body (above about 10 GHz for whole body absorption) and assuming that no power is transmitted through the body, the average absorption cross-section of a homogeneous body will become proportional to the average silhouette (or projected) area $\langle G \rangle$ (Bohren and Huffman 1998):

$$\langle \sigma^a \rangle = \langle Q^a \rangle \langle G \rangle, \tag{4}$$

The proportionality constant is defined as the average absorption efficiency, $\langle Q^a \rangle$, and is related to the average reflection coefficient at the body surface, $\langle |\Gamma|^2 \rangle$, by $\langle Q^a \rangle = 1 - \langle |\Gamma|^2 \rangle$ (Bohren and Huffman 1998). For a tangentially inhomogeneous body the average absorption efficiency will become an average over different tissues layer thicknesses, weighted by the proportion of surface area with each thickness distribution.

For any convex solid object, it can be shown that $\langle G \rangle$ is equal to one quarter of its total surface area (Vouk 1948). This is also an upper bound on $\langle G \rangle$ for a non-convex body (Taylor *et al* 2006). Defining a shadowing factor $0 \le \gamma_s \le 1$ to account for presence of re-entrant rays in the non-convex case we relate $\langle G \rangle$ to *BSA* using

$$\langle G \rangle = \frac{1}{4}\gamma_s\, BSA\ . \tag{5}$$

Average absorption efficiency can then be determined from

$$\langle Q^a \rangle = \frac{4}{\gamma_s}\frac{\langle \sigma^a \rangle}{BSA}\ . \tag{6}$$

The shadowing factor can be estimated as the proportion of the total surface area of the body that is illuminated by the reverberant field. Tomita *et al* (1999) provide data on the distribution of surface area across different body regions. Using their data for a sitting posture and assuming that one third to one half of each arm (7.5 % of BSA) and each leg (17% of BSA) is shadowed we estimate that $\gamma_s \approx 0.75 - 0.85$.

Also in the GO limit, assuming that the absorption efficiency of the body does not vary much over the body surface, we can estimate maximal ACS for frontal illumination with a single vertically polarised plane-wave from the average ACS in a reverberant environment using the ratio of maximum to average silhouette areas

$$\sigma^{a}_{max} \approx \frac{G_{max}}{\langle G \rangle} \langle \sigma^{a} \rangle . \qquad (7)$$

Tomita et al. (1999) also give an empirical linear model for BSA in terms of frontal silhouette area: $BSA = 3.4303\ G_{max} + 0.0033$. Using (5) we can then estimate that $G_{max} / \langle G \rangle \approx 4 / 3.43 / \gamma_s = 1.16 / \gamma_s \approx 1.4 - 1.6$. This ratio is important for aligning worst-case ACS and WBSAR data with average data measured in a reverberation chamber; it is discussed further in Section 5.

3. Methodology

3.1 ACS measurement in reverberation chamber

The measurement technique has been described in detail by Melia (2013) and uses the experimental configuration shown in Figure 1. A screened room (4.70 m × 3.00 m × 2.37 m) acts as a resonant cavity with many modes excited simultaneously; a purpose-built paddle or "mode-tuner" perturbs the field patterns, randomising the directions of incidence to which the subject in the chamber is exposed. The total power injected into the room is low enough to ensure that human exposure is well within international guidelines (ICNIRP 1998).

The measurement parameters were optimised to provide rapid and accurate average ACS measurements (Melia 2013). The measurement time per subject is about seven minutes: A relatively short measurement time is essential so that the subjects can maintain a steady body posture throughout the measurement. At each frequency we obtain the average ACS, and its statistical uncertainty, by the method of Carlberg *et al* (2004). The overall statistical measurement uncertainty was 3 %. The complete measurement system and processing algorithms were validated using a spherical phantom (Melia 2013).

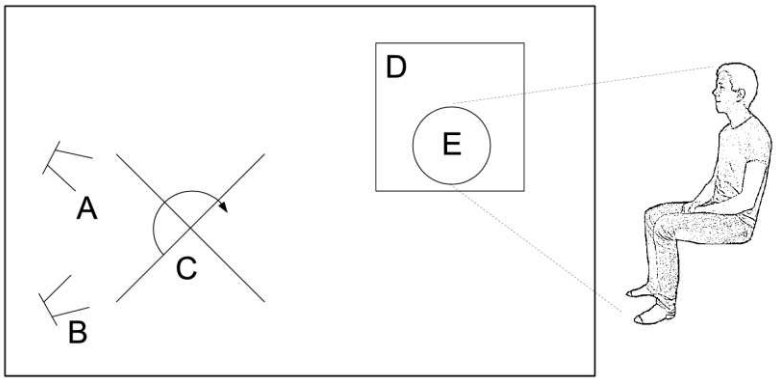

Figure 1. Plan view of the experimental set-up for measuring ACS. Broadband horn antennas (A and B) are connected via coaxial cables and bulkhead connectors to a vector network analyser outside the chamber. A motor in the roof drives the paddle (C) which tunes the modes. Polystyrene blocks (D) provide a seat and keep the feet of the subject (E) at least a quarter-wavelength above the floor. The seated posture depicted on the right was taken by all subjects in the study during the measurement.

Subjects were seated on polystyrene blocks which provide low-permittivity, low-loss support and also fulfil the requirement of keeping the subject's feet a distance of at least $\lambda/4$ from the floor (7.5 cm at 1 GHz). Subjects wore a single layer of light cotton clothing. They were asked to remove shoes and extra clothes, along with the contents of their pockets, metal objects such as belt buckles, and any jewellery. All subjects adopted the same sitting posture, illustrated in Figure 1. This posture was chosen to make it easier for the subjects to minimise movement during the measurement. The effects of variations in body posture and clothing on the ACS measurement have been investigated and quantified (Melia 2013). The systematic errors were estimated as 3 % for posture variation and 2 % for subject clothing. For a male subject of mass 72 kg and height 1.8 m the sitting posture has a 4-17% lower average ACS than a standing "star" posture with arms and legs outstretched over the frequency band 1-12 GHz (Melia 2013). The ACS of a standing posture with legs together and arms by the side is on average about 10 % higher than the chosen sitting posture over then frequency band.

3.2 Human subjects

Sixty adult volunteers (self-selecting) were recruited locally after obtaining ethical permission. The group was not designed to be a representative sample of a particular population, but we did attempt to get a variety of different body types for investigating correlations. There were 36 males and 24 females. Ages ranged from 19-71 years.

Table 1. Summary of the study group population morphological parameters. The normality test gives the p-values of a Shapiro-Wilk test of the null hypothesis that the parameter is normally distributed.

Morphological parameter	**min.**	**median**	**mean**	**max.**	**std. dev.**	**Normality test**
mass, m (kg)	45.8	69.5	72.6	109.5	15.2	0.052
height, h (m)	1.52	1.72	1.73	1.97	0.10	0.36
waist circumference, W (m)	0.61	0.83	0.85	1.16	0.13	0.17
body mass index, BMI (kg m^{-2})	17.0	23.2	24.0	35.6	3.9	0.013
inverse BMI, BMI^{-1} (m^2 kg^{-1})	0.028	0.043	0.043	0.059	0.007	0.95
body surface area, BSA[1] (m^2)	1.43	1.85	1.86	2.36	0.22	0.42
mean fat layer thickness, d_{SF}[a] (mm)	2.3	8.3	8.5	20.4	3.7	0.00047

[a] Estimated from empirical formula.

Table 1 summarises the morphological parameters of the subjects. The primary external morphological parameters measured were mass, m, height, h, and waist circumference, W. Mass was measured with electronic scales (Salter Electronics, Tonbridge), validated against a second balance (MK Scales Ltd, Milton Keynes) showing a difference of less than 0.5 %. Height was measured with a ruler, to a precision of 1 cm and waist circumference was found with a tape measure to a precision of 2 cm. Body mass index (BMI) was obtained from

$$BMI = \frac{m}{h^2}. \tag{8}$$

Surface area is hard to measure directly without special equipment which we did not have, so instead we estimated it from *h* and *m* using the formulas of Tikuisis *et al* (2001):

$$BSA = 0.01281\ m^{0.44}(100\ h)^{0.60} \quad \text{(male)} \tag{9a}$$

$$BSA = 0.01474\ m^{0.47}(100\ h)^{0.55} \quad \text{(female)}\ , \tag{9b}$$

where mass and height are in kg and m. This model is based on a much larger sample of people than the widely used Du Bois-Du Bois formula (Du Bois and Du Bois 1916).

A secondary internal morphological parameter, the mean thickness of the subcutaneous fat layer, was also investigated. The proportion by mass of fat in the body, ζ_{BF}, was estimated from an empirical formula obtained from dual X-ray absorptiometry scans (Gallagher *et al* 2000):

$$\zeta_{BF} = 0.76 + \frac{1.54\ g - 10.978}{BMI} + \left(0.34\ g + 5.3 \times 10^{-4}\right) y\ , \tag{10}$$

where *g* is 1 for male and 0 for female and *y* is age in years. The proportion of this fat, ζ_{SF}, that is subcutaneous is estimated at 0.85 (Thomas *et al* 1998), and its density ρ_{fat} is approximately 900 kg/m^3 (Heymsfield *et al* 2005). Thus by obtaining the volume of subcutaneous fat and dividing by body surface area, we can estimate its average thickness from:

$$\overline{d}_{SF} = \frac{\zeta_{BF}\,\zeta_{SF}\,m}{\rho_{fat}\ BSA}\ . \tag{11}$$

A Shapiro-Wilk normality test on each morphological parameter of the study group rejects the null hypothesis of a normal distribution for *BMI* and d_{SF} (p-value < 0.05). Normality of the distribution of masses is marginally not rejected.

Quantile-quantile plots of the distribution of four of the morphological parameters against reference population data for the United Kingdom are shown in Figure 2 (Ruston *et al* 2004). We have compared to the reference data averaged over all age groups. Compared to this population the study group is somewhat underweight, though height is reasonably well dispersed. The BMI and waist circumference are also correspondingly lower in the sample.

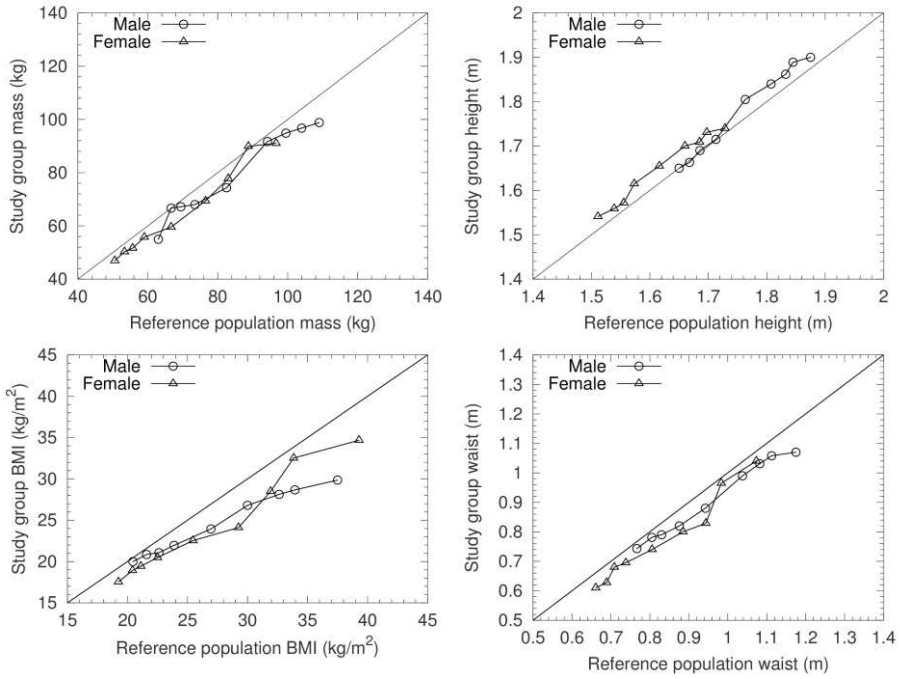

Figure 2. Quantile-quantile plots of the study group morphological parameters compared to UK population data (Ruston *et al* 2004).

4. Results

4.1 Average ACS distribution

Figure 3 shows the average ACS of some of the subjects plotted against frequency. To make the graph clearer we have selected only nine of the subjects, with a range of body masses. As expected, the heavier subjects tend to have a larger ACS. The other subjects showed a similar variation of $\left\langle \sigma^{a} \right\rangle$ with frequency to those in the figure: the average ACS falls with frequency up to 5-8 GHz and then slowly rises again.

Table 2 summarises the main statistical parameters of the measured average ACS in six frequency bands. The values in each band are averaged over a 50 MHz window centred on the band frequency. Overall the average ACS of the adult subjects varied from 0.15 to 0.4 m^2. A Shapiro-Wilk normality test in each band only rejects the null hypothesis of a normal distribution of average ACS at the 5 % significance level in the 3 GHz band.

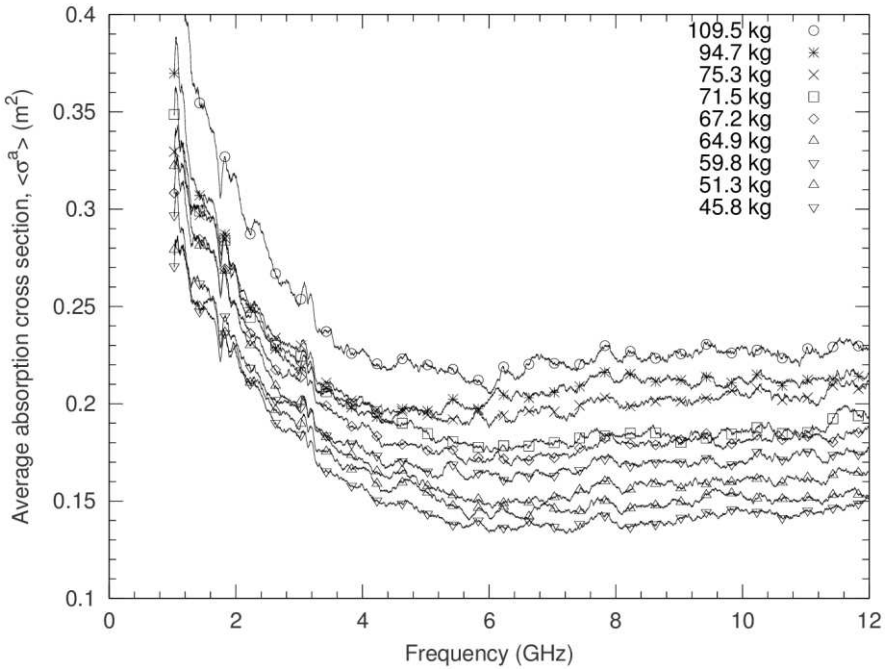

Figure 3. Average ACS of selected subjects versus frequency. The markers are placed at every 200th data point to aid discrimination of the lines.

Table 2. Summary statistics of the measured average ACS in six frequency bands. The normality test gives the p-values of a Shapiro-Wilk test of the null hypothesis that the ACS is normally distributed.

Parameter	**1 GHz**	**3 GHz**	**5 GHz**	**7 GHz**	**9 GHz**	**11 GHz**
Minimum (m^2)	0.27	0.17	0.14	0.13	0.14	0.14
Mean (m^2)	0.33	0.21	0.18	0.17	0.18	0.18
Maximum (m^2)	0.41	0.25	0.22	0.22	0.24	0.23
Standard deviation (m^2)	0.036	0.021	0.022	0.025	0.026	0.025
Normality test (p-value)	0.074	0.034	0.311	0.066	0.152	0.146

We investigated the correlation of average ACS with the morphological parameters mass, height, waist circumference, BMI, estimated body surface area and estimated thickness of subcutaneous fat. Table 3 gives the coefficients of determination (R^2) for single linear regression of average ACS on each parameter. The strongest correlations were with surface area and as expected the correlation is generally greatest at higher frequencies where both the wavelength and the penetration depth are much smaller than typical body dimensions, so the interaction with the EM waves should be primarily a surface effect. Note that the strength of the correlation with BSA may be limited by the use of an empirical model to determine BSA. The maximum error of the linear models on BSA over the study group subjects is -30%/+16%. 90% of the subjects are within about ±15% of the model prediction. Notably, the intercept of the linear model is statistically significant at frequencies below 5 GHz, contrary to the direct proportionality often assumed in surrogate models at these frequencies (El Habachi *et al* 2010). Note that on physical grounds we would expect that average ACS becomes directly proportional to average silhouette area and therefore BSA in the GO limit. In particular this means that the direct proportionality will only be valid for BSAs above a threshold at which the body is large enough for the GO approximations to hold true. The onset of this behaviour at about 5 GHz is consistent with the GO view of whole body absorption since the body's main radii of curvature (those corresponding to the main areas of absorption) will not be smaller than a wavelength at frequencies below 5 GHz.

Strong correlations were also found between average ACS and body mass. In particular at 1 GHz the correlation with mass is slightly higher than for BSA. Correlations with linear body scale parameters (height and waist) were a little weaker and the correlation with BMI was poor in all but the 1 GHz band.

Table 3. Coefficient of determination for single linear regression of average ACS against mass, height, waist circumference and estimated BSA in different frequency bands. Figures in parentheses have coefficients with *p*-values greater than 0.05. The strongest correlation in each band is shown in bold. The right columns give the coefficients of the linear model against BSA, normalised by a factor of four to give the average absorption efficiencies with γ_s=1.

f (GHz)	Coefficient of determination, R^2							Linear model for ACS on BSA $\langle\sigma^a\rangle=\alpha+¼\langle Q^a\rangle$ *BSA*	
	mass	**height**	**waist**	**BMI**	**BMI^{-1}**	**BSA**[a]	d_{SF}[a]	α (m^2)	$\langle Q^a\rangle$ (-)
1	**0.82**	0.34	0.74	0.58	0.62	0.77	(0.22)	0.064±0.019	0.58±0.04
3	0.49	**0.61**	0.45	0.13	0.16	0.59	(5×10^{-3})	0.071±0.015	0.30±0.03
5	0.66	0.66	0.56	0.22	0.26	**0.74**	(7×10^{-4})	(0.018±0.013)	0.34±0.03
7	0.72	0.69	0.59	0.25	0.30	**0.80**	(3×10^{-3})	(-0.018±0.013)	0.41±0.03
9	0.73	0.66	0.61	0.27	0.32	**0.81**	(7×10^{-3})	(-0.017±0.013)	0.42±0.03
11	0.73	0.65	0.62	0.28	0.32	**0.80**	(7×10^{-3})	(-0.008±0.013)	0.41±0.03

[a] Estimated from empirical formula.

Step-wise multiple linear regression models for average ACS using different sets of predictor variables were investigated. Generally it was found that if mass and height are included in the regression then adding waist circumference or BSA (which may be expected to have some co-linearity with mass and height) does not improve the coefficient of determination. Very similar coefficients of determination can be obtained using mass and height or BSA and BMI in the regression and gender usually has a beneficial effect. Since BSA was estimated from an empirical formula and is difficult to measure, the regression on height, mass and gender is potential more robust and practically useful and is presented in Table 4.

Table 4. Multiple linear regression of average ACS on height, mass and gender (denoted by *g* and defined as 1 for male and 0 for female) in different frequency bands. Figures in parentheses have coefficients with *p*-values greater than 0.05.

f (GHz)	$\langle\sigma^a\rangle=\alpha+\beta_m m+\beta_h h+\beta_g g$				
	R^2	α (m^2)	β_m (m^2/kg)	β_h (m)	β_g (m^2)
1	0.82	0.218±0.049	0.00221±0.00018	(-0.028±0.033)	(0.0029±0.0056)
3	0.78	0.071±0.033	0.00044±0.00012	0.055±0.022	0.020±0.004
5	0.86	(0.028±0.026)	0.00067±0.00010	0.052±0.018	0.017±0.003
7	0.90	(-0.010±0.026)	0.00087±0.00010	0.065±0.018	0.017±0.003
9	0.89	(0.001±0.027)	0.00094±0.00010	0.058±0.018	0.017±0.003
11	0.88	(0.015±0.028)	0.00092±0.00010	0.052±0.018	0.016±0.003

4.2 Whole-body SAR

The equivalent average WBSAR for each subject was determined from $\langle \text{WBSAR} \rangle = S^i \langle \sigma^a \rangle / m$, taking the incident power density as the ICNIRP reference level of 10 W m^{-2} in the 2-10 GHz band. The quantiles of the average WBSAR distributions obtained

are shown in Figure 4. A Shapiro-Wilk normality test in each band marginally rejects the null hypothesis of a normal distribution of average WBSAR at the 5 % significance level in the 3 GHz band. For comparison the ICNIRP basic restriction on worst-case WBSAR for public exposure below 10 GHz is 0.08 W kg^{-1} (ICNIRP 1998). At 2 GHz, where the ICNIRP reference level tends to be least conservative, the maximum average WBSAR measured was about 60 % of the basic restriction (note that the reference level is reduced according to a linear tapered below 2 GHz). Allowing a worst-case to average ratio of 1.6 the maximum worst-case WBSAR in the study group at 2 GHz is below the basic restriction.

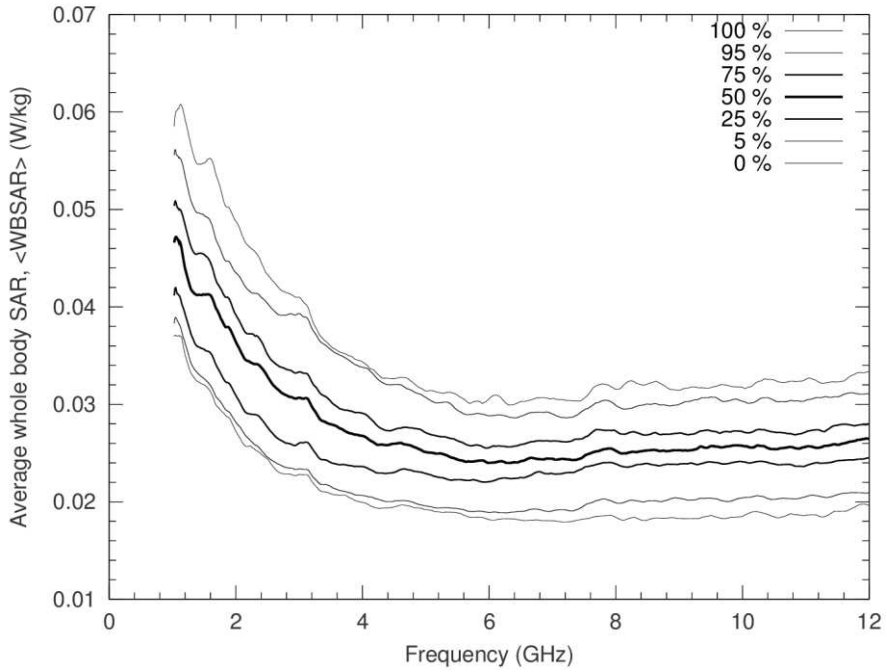

Figure 4. Measured quantiles of the average WBSAR distribution of the subjects at each frequency. The incident power density is 10 Wm^{-2}.

Table 5. Coefficient of determination for single linear regression of average WBSAR against mass, height, waist circumference, BSA, BMI, inverse BMI and estimated mean subcutaneous fat thickness in different frequency bands. Figures in parentheses have p-values greater than 0.05. The strongest correlation in each band is shown in bold. The right columns give the coefficients of the linear model against inverse BMI.

f (GHz)	Coefficient of determination, R^2							Linear model for $\langle WBSAR \rangle$ on BMI^{-1} $\langle WBSAR \rangle = \alpha + \beta\, BMI^{-1}$	
	mass	height	waist	BMI	BMI^{-1}	BSA[a]	d_{SF}[a]	α (W kg^{-1})	β (W m^{-2})
1	**0.82**	0.44	0.53	0.52	0.57	0.83	0.17	0.0184±0.0033	0.66±0.08
3	0.75	0.17	0.50	0.73	**0.77**	0.66	0.50	(0.0034±0.0019)	0.62±0.04
5	0.69	0.12	0.45	0.74	**0.76**	0.59	0.57	0.0066±0.0014	0.43±0.03
7	0.56	0.05	0.37	**0.71**	**0.71**	0.46	0.65	0.0092±0.0013	0.36±0.03
9	0.58	0.06	0.37	**0.70**	**0.70**	0.48	0.62	0.0098±0.0013	0.36±0.03
11	0.62	0.08	0.40	0.70	**0.71**	0.52	0.60	0.0093±0.0014	0.38±0.03

[a] Estimated from empirical formula.

Table 5 gives the coefficient of determination for a linear regression of average WBSAR against each morphological parameter. The strongest correlation at 3 GHz and above is with inverse BMI, though the correlation with BMI itself is only slightly weaker. There is a moderate correlation with mass at all frequencies. The maximum error of the linear model on

inverse BMI over the study group subjects is -25%/+20%. 90% of the subjects are within about ±13% of the model prediction at 2 GHz and above.

4.3 Absorption efficiency

Average absorption efficiency, calculated from equation (6), is plotted against frequency for all subjects in Figure 5, taking $\gamma_s = 1$. The plots necessarily follow the same frequency-dependence as those of average ACS. The spread of values at each frequency point, particularly at frequencies above 8 GHz, is indicative of the real variability in absorption efficiency of the subjects. Figure 6 shows the statistical distribution functions of absorption efficiency in the different frequency bands. A Shapiro-Wilk normality test on the distribution of absorption efficiency does not reject the null hypothesis (p-value < 0.05) of a normal distribution in any frequency band. There appears to be a potential outlier in the $\langle Q^a \rangle$ data – one subject has particularly low absorption efficiency, especially above 6 GHz. The outlier is 3.6 standard deviations from the mean at 9 GHz. A Grubbs test rejects the null hypothesis that there is no outlier (p-value < 0.05) for the 7-11 GHz bands. Since the study group data was anonymised further investigation of this subject was not possible. Since the same subject's ACS is not identified as an outlier in the lower frequency bands and all the data was collected simultaneously the outlier was not removed from any of the data analysis in this paper.

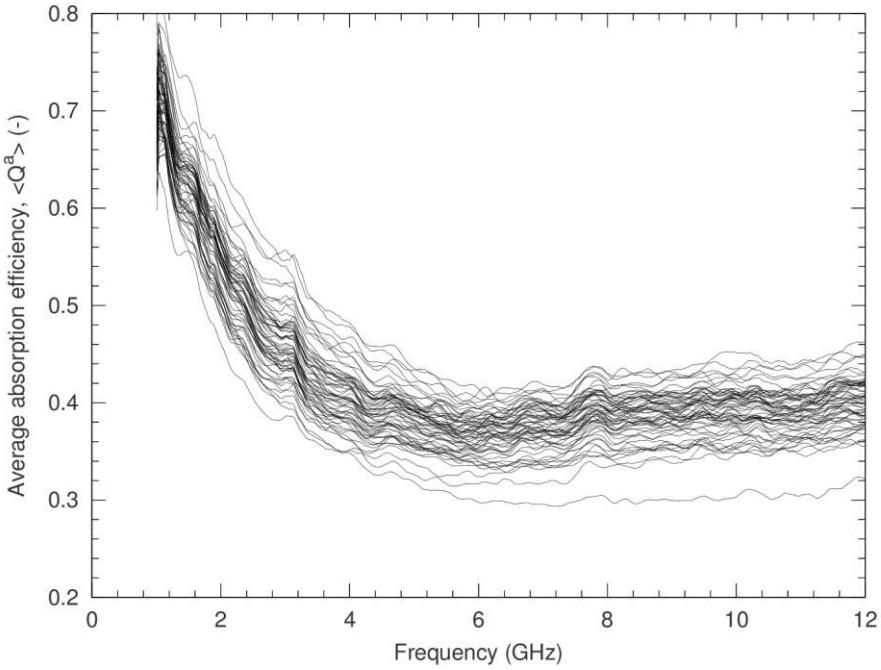

Figure 5. Average absorption efficiency versus frequency for all subjects (γ_s=1).

The absorption efficiency was correlated with morphological parameters in each frequency band. Table 6 gives the coefficient of determination for each parameter. Above 3 GHz the only statistically significant correlation (p-value < 0.05) with $R^2 > 0.2$ is with estimated subcutaneous fat thickness. Hirata *et al* (2010) have previously correlated worst-case WBSAR with body fat percentage at the whole-body resonant frequency. The overall absorption coefficient of the body surface is highly dependent on reflections between the layers of tissues at these frequencies. At 1 GHz the strongest correlation is with height while at 3 GHz there is some correlation with BMI.

Table 6 also gives the linear model coefficients for regression of $\langle Q^a \rangle$ on d_{SF} assuming γ_s=1. A model for the average ACS data based on estimated BSA and subcutaneous fat thickness can be formed from this regression and BSA:

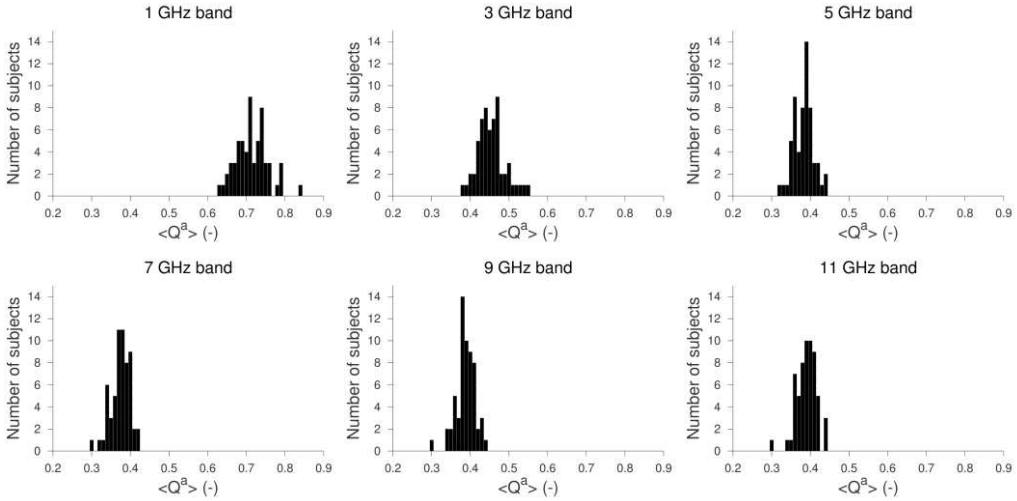

Figure 6. Distribution of average absorption efficiency, $\langle Q^{a} \rangle$ (γ_s=1).

Table 6. Coefficient of determination for single linear regression of estimated average absorption efficiency (γ_s=1) against mass, height, waist circumference, BSA, BMI, inverse BMI and estimated mean subcutaneous fat thickness in different frequency bands. Figures in parentheses have corresponding coefficients with p-values greater than 0.05. The strongest correlation in each band is shown in bold. The right columns give the coefficients of the linear model against d_{SF}.

f (GHz)	Coefficient of determination, R^2							Linear model for $\langle Q^a \rangle$ on d_{SF} $\langle Q^a \rangle = \alpha + \beta\, d_{SF}$	
	mass	height	waist	BMI	BMI^{-1}	BSA[a]	d_{SF}[a]	α (-)	β (mm^{-1})
1	0.10	**0.31**	0.01	10^{-4}	10^{-3}	0.16	0.02	0.700±0.013	(0.0017±0.0015)
3	0.27	0.03	0.12	0.32	0.33	0.22	**0.40**	0.507±0.009	-0.0061±0.0010
5	0.04	0.01	0.00	0.13	0.11	0.02	**0.33**	0.417±0.007	-0.0040±0.0007
7	0.01	0.15	0.05	0.02	0.01	0.03	**0.26**	0.403±0.007	-0.0034±0.0008
9	0.01	0.11	0.06	0.01	0.003	0.03	**0.20**	0.414±0.007	-0.0030±0.0008
11	0.00	0.07	0.03	0.03	0.02	0.007	**0.24**	0.419±0.007	-0.0034±0.0008

[a] Estimated from empirical formula.

$$\left\langle \sigma^{a} \right\rangle = \frac{1}{4} BSA \quad (\alpha + \beta\, d_{SF}) . \tag{12}$$

The maximum relative error between the predictions of this model and the measured average ACS for each subject in the study group is -23% / +17%. 90% of the subjects are within ±12% of the model prediction. This is only a slight improvement on the linear model for average ACS based directly on BSA.

Since females generally have higher body fat percentages than males it is interesting to compare how the measurement results vary between genders (Figure 7). The average ACS of female subjects is generally lower than that of males in all the frequency bands, particularly at the higher frequencies. This is to be expected from the generally smaller body size of females. When the average absorbed power is normalised by BSA as absorption efficiency

the trend is different. Females have slightly higher absorption efficiency in the 1 GHz band and lower at 5 GHz and above. In the 3 GHz band the absorption efficiencies are very similarly distributed. When the average absorbed power is normalised by mass as average WBSAR there is little difference between males and females at 3 GHz and above – the lower absorption of females is compensated by their lower mass. However, at 1 GHz females generally have higher WBSAR.

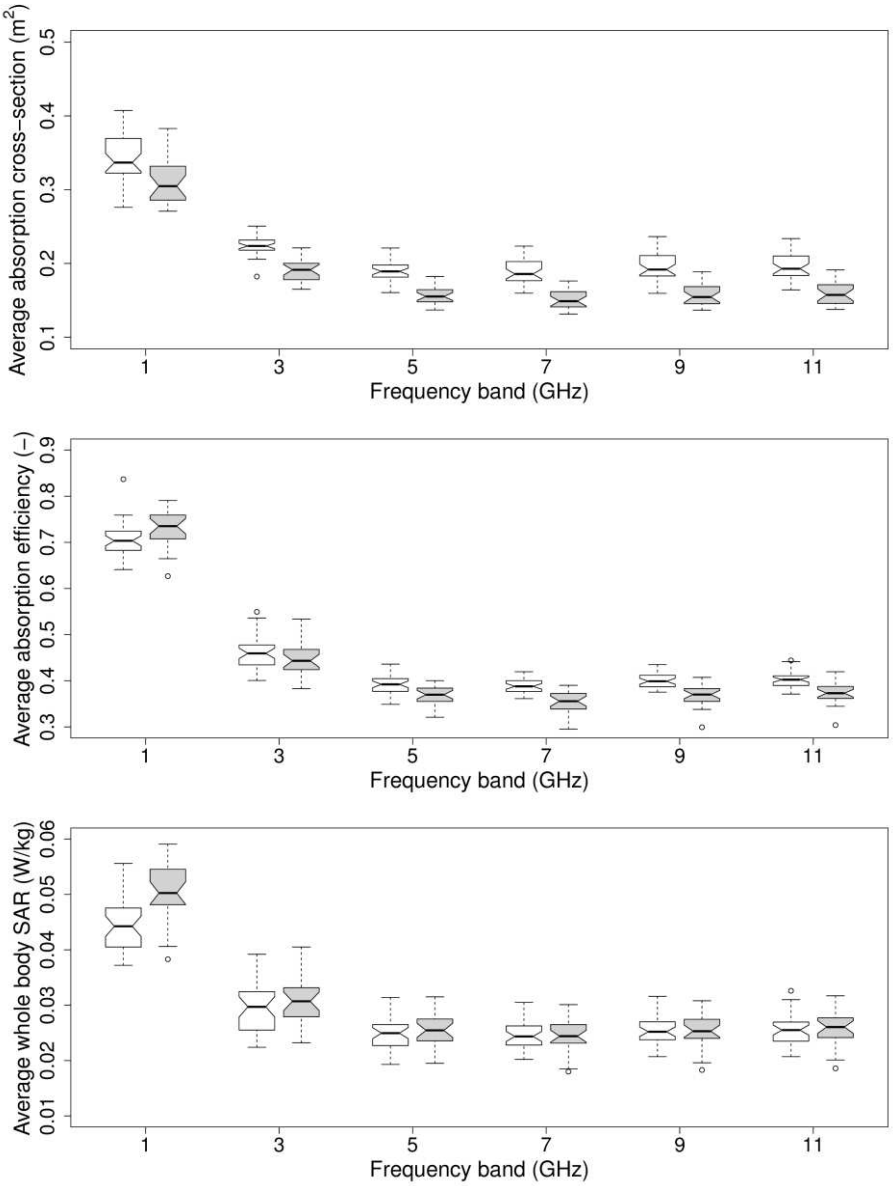

Figure 7. Gender dependency of average ACS (top), average absorption efficiency (middle) and average WBSAR (bottom) depicted as notched boxplots in each frequency band. Male subjects are shown on the left of each band with white boxes and female subjects on the right with grey boxes. Data points marked with circles are outside 1.5 times the interquartile range.

5. Comparison and discussion

There are few reported studies, either experimental or numerical, that determine ACS averaged over polarisation and angle of incidence directly or provide enough information to calculate it indirectly without assumptions about worst-case to average ratios or the angular dependence. Table 7 summarises how the average ACS from these studies compares to our

measured values. Our previous study (Melia *et al* 2013) measured the average ACS of 9 subjects at 1-8.5 GHz with less accuracy than the present study. Figure 8 shows the average ACS of the homogeneous and heterogeneous male phantoms in Uusitupa *et al* (2010) compared to the measured average ACS of subjects of similar mass. An unweighted average of the ACS values for different directions of incidence and polarisations reported by Uusitupa *et al* is biased due to the non-uniformity of the directions sampled. An unbiased estimate of the average ACS was determined using a weighted average based on an ellipsoidal model for the silhouette area as a function of direction as described in Melia *et al* (2012). The unbiased average for the heterogeneous phantom is in good agreement with the measurement data. Using this unbiased estimate of the average the ratio of worst-case to average ACS/WBSAR can also be estimated from the heterogeneous phantom data in Uusitupa *et al* as 1.8 at 300 MHz and about 1.6 at 500 MHz and above. This result is consistent with the observation of Harima (2012), that the WBSAR of a single adult male in a reverberation chamber was approximately 50% of the worst-case WBSAR. This ratio is used to align worst-case and average ACS/WBSAR data below.

Table 7. Comparison of our measured average ACS to literature values of average ACS at 1-9 GHz. Rows in bold indicate cases in which our measured range of ACS does not overlap (or does so only marginally) with the literature values.

Frequency, *f* (GHz)	**This study**	**Literature results**		
	$\langle\sigma^a\rangle$ full range (m^2)	**$\langle\sigma^a\rangle$ (m^2)**	**measured (m) simulated (s)**	**Reference**
1.0	0.27-0.41	0.28-0.47	m	a
1.0	0.27-0.41	0.33	m	b
1.0	0.27-0.41	0.39	m	c
1.0	0.27-0.41	0.54	m (grounded)	g
1.5	0.24-0.35	0.37	m	c
2.0	0.21-0.32	0.30	m	c
2.0	0.21-0.32	0.44	m (grounded)	g
2.1	0.20-0.30	0.21-0.47	s	d
2.3	**0.19-0.29**	**0.28-0.42**	**m**	**e**
2.5	0.18-0.28	0.20	m	b
3.0	**0.17-0.25**	**0.24-0.43**	**m**	**e**
3.0	0.17-0.25	0.34	m (grounded)	g
3.5	0.15-0.24	0.18-0.23	m	a
3.5	0.15-0.24	0.16-0.37	s	d
4.0	**0.15-0.23**	**0.11**	**m**	**b**
4.0	0.15-0.23	0.30	m (grounded)	g
5.0	0.14-0.22	0.12-0.31	s	d
5.0	0.14-0.22	0.27	m (grounded)	g
3.0-8.0 (mean 5.5)	**0.14-0.22**	**0.33**	**m**	**f**
6.0	0.13-0.21	0.12-0.19	m	a
6.0	0.13-0.21	0.28	m (grounded)	g
7.0	0.13-0.22	0.28	m (grounded)	g
8.0	0.14-0.23	0.32	m (grounded)	g
8.5	0.14-0.23	0.13-0.22	m	a

References: a, Melia *et al* (2013); b, Harima (2012); c, Wang *et al* (2012); d, Uusitupa *et al* (2010); e, Bamba *et al* (2012); f, Andersen *et al* (2012); g, Senic *et al* (2013).

Other measurements using reverberant techniques at frequencies up to 4 GHz have been presented by Bamba *et al* (2012), Wang *et al* (2012), Harima (2012) and Senic *et al* (2013). Values averaged over a very broad range of 3-8 GHz have been obtained by Andersen *et al* (2012). Our average ACS results are in good agreement with the measured average ACS of Wang (2012) and Harima (2012), but generally lower than the measured average ACS of both Bamba *et al* (2012) and Andersen *et al* (2012). The latter two studies were designed to estimate in-situ ACS in real environments with both direct line-of-sight (LOS) and non-uniform diffuse fields incident on the subjects. Andersen *et al* (2012) find ACS varies from 0.24 m^2 to 0.36 m^2 depending on the antenna locations, which is indicative of the non-ideal

reverberant environment used in their study. More recently the same authors have quantified the relative contribution of stochastic and non-stochastic components to the estimated WBSAR (Bamba *et al* 2013). In our measurements the non-stochastic contributions to the ACS have been minimised to give an accurate determination of the average ACS (Melia 2013). Senic *et al* (2013) measured the ACS of a single subject of mass 72.5 kg and height 1.79 m over 0.2-8 GHz with an estimated statistical error of about 13%, however their subject was grounded so the results are not directly comparable: The average ACS of their grounded subject is typically 50 % higher than the median of our ungrounded subjects, which is somewhat higher than the typical increase of in ACS at the resonant frequency of 10 % found for worst–case WBSAR for grounded versus ungrounded phantoms in numerical simulations (Hirata *et al* 2012).

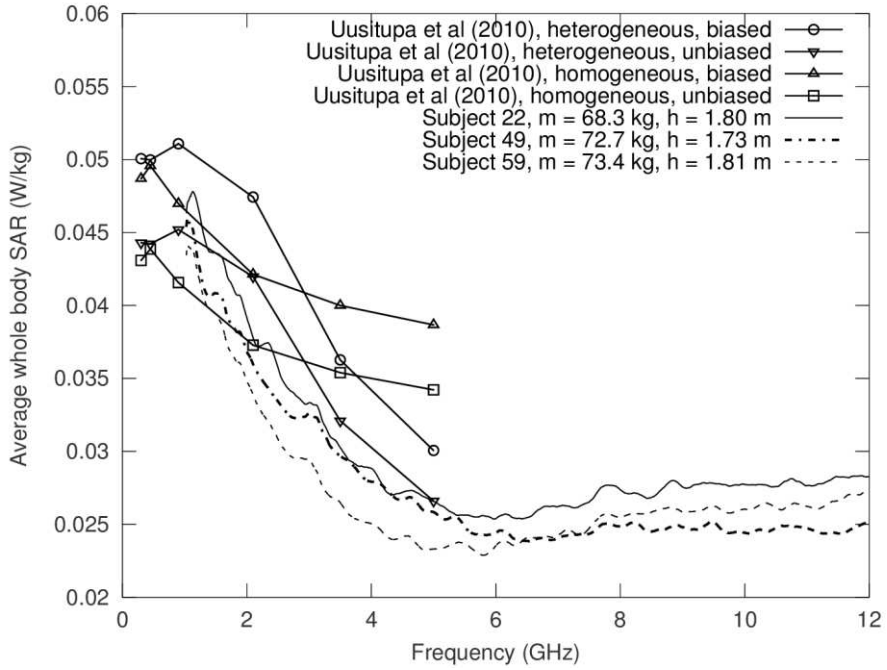

Figure 8. Comparison of average ACS calculated from the data in Uusitupa *et al* (2010) to the most closely matched (in mass) male subjects from our study. Data for both the heterogeneous (mass 72.24 kg) and homogeneous (mass 68.55 kg) male phantoms are shown using both un-weighted biased and weighted unbiased averages as described in the text.

Hirata *et al* (2007) have investigated the correlation between ACS and body surface area for humans at far field exposure using numerical phantoms: A linear fit of their simulated worst-case ACS to BSA at 2 GHz gave $\sigma^a / BSA = 0.196$. El Habachi *et al* (2010) calculated this ratio at 2.1 GHz using the Japanese Male, Zubal, Visible Human, Korean and Norman phantoms. They find $m \cdot WBSAR / BSA = \sigma^a / BSA = 0.17 - 0.28$ with $R^2 = 0.92$-0.99 at 2 GHz, depending on which family of numerical phantoms is used. The linear model of our ACS data has a statistically significant intercept in the relationship between BSA and ACS at frequencies below 5 GHz. At 2 GHz the linear model of our data is $\langle \sigma^a \rangle = (0.090 \pm 0.015) + (0.089 \pm 0.008) BSA$ (p-value < 10^{-8}) with R^2=0.69. Forcing our data to an intercept of zero we obtain $\langle \sigma^a \rangle = (0.135 \pm 0.01) BSA$ (p-value < 10^{-16}). Assuming a worst-case to average ACS ratio of 1.6, as determined from data in Uusitupa *et al* (2010) above, we can align the models for worst-case ACS found by Hirata *et al* (2007) and El Habachi *et al* (2010) with our average ACS models as shown in Figure 9. While the exact relationship between worst-case and average ACS is likely to depend somewhat on body

shape this scaling allows the dispersion of the measured data to be assessed against the literature worst-case data. The overall dispersion of our measurement results is bounded by the range of the linear models over the different phantom families found by El Habachi *et al* (2010), however, its range at each BSA is generally less than that across all the phantoms. Our data is quite centralised with the models of El Habachi *et al* (2010) using a worst-case to average ratio of 1.6 and a little lower than the model for NORMAN which is based on a subject from the same population as the subjects in the study.

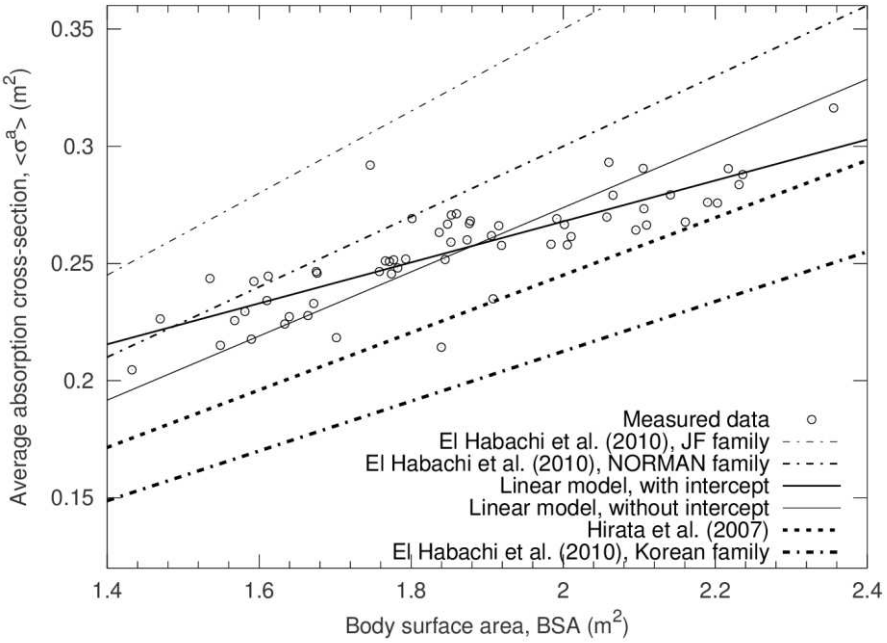

Figure 9. Comparison of our linear model of ACS against BSA at 2 GHz to Hirata *et al* (2007) and El Habachi *et al* (2010). The literature worst-case ACS values are scaled down by a factor 1.6 to compare to our average ACS.

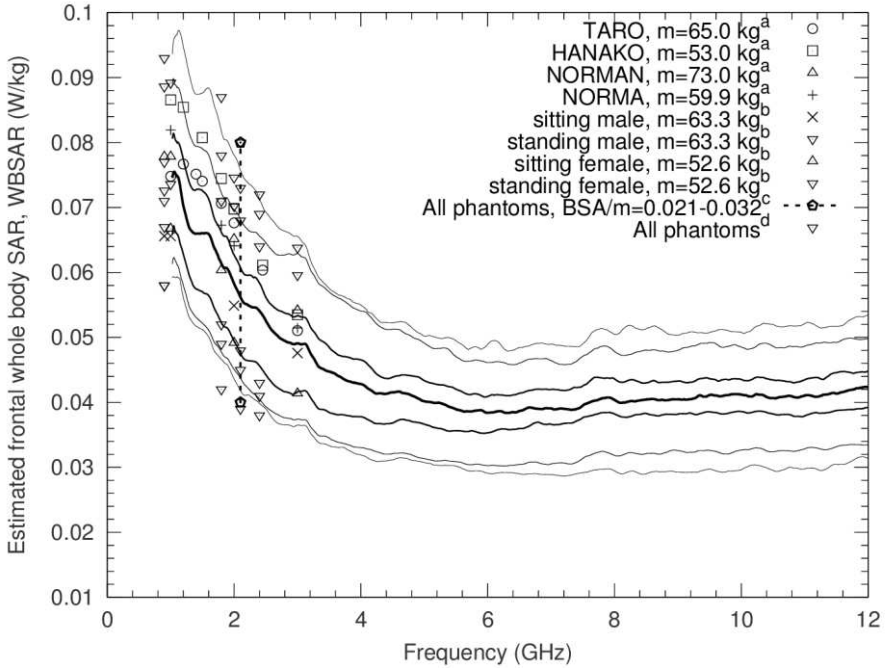

Figure 10. Estimated quantiles (0%, 5% , 25%, 50%, 75%, 95%, 100%) of the worst-case WBSAR distribution compared to literature results: [a] Dimbylow *et al* (2008);

[b] Nagaoka and Watanabe (2008); [c] El Habachi *et al* (2010); [d] Conil *et al* (2008). The worst-case WBSAR of each subject is assumed to be 1.6 times higher than the measured average value at all frequencies to allow comparison of the dispersion between our measurements and literature values. A vertical line indicates a range with markers at the extreme values.

In order to compare our average WBSAR data with the literature on worst-case WBSAR we have again scaled the average WBSAR of each individual by a factor of 1.6 at every frequency. Figure 10 shows this comparison for some recent numerical phantom studies. For El Habachi *et al* (2010) we have shown the range of average WBSAR across all the phantoms for BSAs over the range of our study group. This data aligns well with the measurements using the worst-case to average scaling ratio of 1.6. Generally the numerical simulation results are well dispersed amongst the quantiles of the measurement data. At 2 GHz the highest estimated worst-case WBSAR was 0.078 W/kg for a 20 year-old female subject with mass 45.8 kg and height 1.64 m, which us just below the ICNIRP basic restriction.

El Habachi *et al* (2010) find R^2=0.88-0.95 for linear regression of worst-case WBSAR against inverse BMI at 2.1 GHz across six numerical phantom families with a linear coefficient of 1.1-1.6 (renormalized for 10 Wm^{-2} incident power). This compares to our R^2 of 0.78 across the whole study group at 2 GHz. We find a linear coefficient of 0.72±0.05 (p-value 4×10^{-12}) for average WBSAR with a non-zero intercept of 0.0187±0.0033 (p-value 3×10^{-7}). Assuming a worst-case to average WBSAR ratio of 1.6 these models are consistent for BMI^{-1} greater than about 0.04 while our model gives somewhat higher WBSAR at lower BMI^{-1} (50% higher at BMI^{-1} =0.02). This could be due to our study group being a somewhat underweight sample of the population. The negative correlation of average absorption cross-section with mean subcutaneous fat thickness above 1 GHz is broadly consistent with Hirata *et al*'s (2010) finding at the whole-body resonance frequency, however, at 1 GHz we do not find a statistically significant linear coefficient. Note that Hirata et al's correlation with body fat percentage is normalised to inverse BMI whereas our correlation with mean fat thickness is normalised to surface area.

Sandrini *et al* (2004) compared the worst-case WBSAR in grounded male and female phantoms from 0.1 to 4 GHz, though only using three male and two female phantoms. The results suggested higher worst-case WBSAR for females at 1-4 GHz. Our statistical distributions for average WBSAR of ungrounded subjects would only support higher WBSAR for females at 1 GHz; at 3 GHz and above the distributions of average WBSAR across the study group are very similar between males and females.

6. Conclusions

We have applied a fast, accurate and repeatable technique to measure the ACS, averaged over polarisation and angle of incidence, of 60 adult subjects at microwave frequencies of 1-12 GHz. This includes the 5-10 GHz band in which little data on ACS/WBSAR has been reported. We have shown how the average ACS varies with frequency and have demonstrated that it correlates well with body surface area, but that it only becomes directly proportional to BSA at 5 GHz and above. Average WBSAR correlates most strongly with inverse BMI at 3 GHz and above. We have also shown that the average absorption efficiency correlates most strongly with the estimated average fat layer thickness of the subjects out of all the morphological parameters considered.

Surrogate linear models for average ACS in terms of BSA, average WBSAR in terms of inverse BMI and average absorption efficiency in terms of mean fat thickness have been determined and compared to those determined from numerical phantom simulations. Our models cover a broader frequency range than previous studies and are based on a larger sample population of distinct individuals covering a wide range of morphologies. The

maximum relative errors in our linear models at 2 GHz of ACS against BSA (-30%/+16%) and WBSAR against BMI^{-1} (-25%/+20%) are consistent with the observation of El Habachi *et al* (2010) that the relative error in surrogate models based on one external morphological parameter in numerical simulations is about 30%. The maximum relative error (-23/+17%) of the model based on estimated mean fat layer thickness was only marginally smaller, however, this model itself used an empirical model for fat mass determined from only external parameters.

We have compared the measurement results to the few other studies of average ACS/WBSAR and using a worst-case to average ratio estimated from the scaling behaviour in the high frequency limit (that is consistent with that found in numerical phantom studies) we have semi-quantitatively compared our average ACS results to the much broader literature on worst-case WBSAR. The maximum estimated worst-case WBSAR in the study group was at 2 GHz and was marginally below the ICNIRP basic restriction for exposure at the reference level. The dispersion of average ACS and WBSAR in the study group is generally consistent with the dispersion found from numerical simulation across multiple phantom families. However, being based on measurements of 60 real subjects - including the effects of variations in body shape, electrical parameters of tissues and internal anatomy - our results provide for the first time direct quantitative evidence of the variation in ACS and WBSAR across a real population. This opens the way for human exposure assessments made using particular numerical phantoms to be accurately calibrated for a particular population and also allows the position of reference levels to be quantified with respect to exposure variations due to morphological variations.

The technique could in principle be extended to lower frequencies if suitable antennas, network analyser and screened room were available. Extending down in frequency to encompass more of the mobile communication bands at 0.8-1 GHz is particularly desirable, though for much lower frequencies, the room would need to be larger in order to provide enough cavity resonances for a good reverberant environment.

Acknowledgment

The research leading to these results has received funding from the European Community's Seventh Framework Programme (FP7/2007-2013) under grant agreement no. 205294.

References

Andersen J B, Chee K L, Jacob M, Pedersen G F and Kürner T 2012 Reverberation and absorption in an aircraft cabin with the impact of passengers *IEEE Trans. Antennas and Propagation* **60** 2472–2480

Bamba A, Joseph W, Andersen J B, Tanghe E, Vermeeren G, Plets D, Nielsen J Ø and Martens L 2012 Experimental assessment of specific absorption rate using room electromagnetics *IEEE Trans. Electromag. Compat.* **54** 747–757

Bamba, A, Joseph W, Vermeeren G, Tanghe E, Gaillot D P, Andersen J B, Nielsen J Ø, Lienard M and Martens L 2013 Validation of experimental whole-body SAR assessment method in a complex indoor environment *Bioelectromagnetics*, **34**(2) 122-132

Bohren C F and Huffman D R 1998 Absorption and Scattering of Light by Small Particles *John Wiley & Sons*

Carlberg U, Kildal P-S, Wolfgang A, Sotoudeh O and Orlenius C 2004 Calculated and measured absorption cross sections of lossy objects in reverberation chamber *IEEE Trans. Electromag. Compat.*, **46**(2) 146 – 154

Conil E, Hadjem A, Lacroux F, Wong M F and Wiart J 2008 Variability analysis of SAR from 20 MHz to 2.4 GHz for different adult and child models using finite-difference time-domain *Phys. Med. Biol.* **53** 1511–1525

Conil E, Hadjem A, Gati A, Man-Fai Wong and Wiart, J 2011 Influence of plane-wave incidence angle on whole body and local exposure at 2100 MHz *IEEE Transactions on Electromagnetic Compatibility* **53**(1) 48-52

Du Bois D and Du Bois E F 1916 A formula to estimate the approximate surface area if height and weight be known *Arch. Intern. Med.* **17** 863–871

Dimbylow P J, Hirata A and Nagaoka T 2008 Intercomparison of whole-body averaged SAR in European and Japanese voxel phantoms *Phys. Med. Biol.* **53** 5883-5897

El Habachi A, Conil E, Hadjem A, Vazquez E, Wong M F, Gati A, Fleury G and Wiart J 2010 Statistical analysis of whole-body absorption depending on anatomical human characteristics at a frequency of 2.1 GHz *Phys. Med. Biol.* **55**(7) 1875–1887

Findlay R P and Dimbylow P J 2005 Effects of posture on FDTD calculations of specific absorption rate in a voxel model of the human body *Phys. Med.Biol.* **50** 3825-3835

Gallagher D, Heymsfield S B, Heo M, Jebb S A, Murgatroyd P R and Sakamoto Y 2000 Healthy percentage body fat ranges: an approach for developing guidelines based on body mass index *The American Journal of Clinical Nutrition* **72**(3) 694-701

Hand J W 2008 Modelling the interaction of electromagnetic fields (10 MHz–10 GHz) with the human body: methods and applications *Phys. Med. Biol.* **53** R243-R286

Harima K 2012 Estimation of power absorbed by human body using reverberation chamber *IEEE Symposium on Electromagnetic Compatibility* (Pittsburgh, PA, USA) 5-12 Aug.

Heymsfield S B, Lohman T G, Wang Z M and Going S B (editors) 2005 *Human Body Composition* 2nd edition. Human Kinetics Publishers, Champaign, IL, USA

Hill D A 2009 Electromagnetic fields in cavities: Deterministic and statistical theories *IEEE Press*

Hirata A, Nagaya Y, Osamu F, Nagaoka A T and Watanabe S 2007 Correlation between absorption cross section and body surface area of human for far-field exposure at GHz bands *EMC 2007. IEEE International Symposium on Electromagnetic Compatibility*, July 9-13 (Honolulu, HI, USA) 1-4

Hirata A, Ito N, Fujiwara O, Nagaoka T and Watanabe S 2008 Conservative estimation of whole-body-averaged SARs in infants with a homogeneous and simple-shaped phantom in the GHz region *Phys. Med. Biol.* **53** 7215-7223

Hirata A, Fujiwara O, Nagaoka T and Watanabe S 2010 Estimation of whole-body average SAR in human models due to plane-wave exposure at resonance frequency *IEEE Transactions on Electromagnetic Compatibility*, **52**(1) 41-48

Hirata A, Yanase K, Laakso I, Chan K H, Fujiwara O, Nagaoka T, Watanabe S, Conil E and Wiart J 2012 Estimation of the whole-body averaged SAR of grounded human models for plane wave exposure at respective resonance frequencies *Phys. Med. Biol.* **57** 8427-8442

ICNIRP 1998 Guidelines for limiting exposure to time-varying electric, magnetic and electromagnetic fields (up to 300 GHz) *Health Phys.* **44** 1630–1639

Melia G C R, Flintoft I D and Robinson M P 2012 Absorption cross-section of the human body in a reverberant environment *2012 International Symposium on Electromagnetic Compatibility (EMC Europe)*, Roma, 17-21 Sept.

Melia G C R 2013 Electromagnetic Absorption by the Human Body *PhD Thesis* Department of Electronics, University of York

Melia G C R, Robinson M P, Flintoft I D, Marvin A C and Dawson J F 2013 Broadband measurement of absorption cross-section of the human body in a reverberation chamber *IEEE Trans. Electromag. Compat*. **55** 1043-1050

Nagaoka T and Watanabe S 2008 Postured voxel-based human models for electromagnetic dosimetry *Phys. Med. Biol.* **53** 7047-7061

Neubauer G, Preiner P, Cecil S, Mitrevski N, Gonter J and Garn H 2009 The relation between the specific absorption rate and electromagnetic field intensity for heterogeneous exposure conditions at mobile communications frequencies *Bioelectromagnetics* **30**(8) 651-662

Ruston D, Hoare J, Henderson L, Gregory J, Bates C J, Prentice A, Birch M, Swan G and Farron M 2004 The National Diet & Nutrition Survey: Adults aged 19 to 64 years *TSO* London ISBN 0 11 621569 0.

Sandrini L, Vaccari A, Malacarne C, Cristoforetti L and Pontalti R 2004 RF dosimetry: a comparison between power absorption of female and male numerical models from 0.1 to 4 GHz *Phys. Med. Biol.* **49** 5185-5201

Senic D, Sarolic A and Joskiewicz Z M 2013 Preliminary results of human body average absorption cross section measurements in reverberation chamber *2013 International Symposium on Electromagnetic Compatibility (EMC EUROPE),* Brugge, Belgium, 2-6 Sept. 887-890

Taylor M A, Garboczi E J, Erdogan S T and Fowler D W 2006 Some properties of irregular particles in 3-D *Powder Technology* **162** 1-15

Thomas E L, Saeed N, Hajnal J V, Brynes A, Goldstone A P, Frost G and Bell J D 1998 Magnetic resonance imaging of total body fat *Journal of Applied Physiology* **85**(5) 1778-1785

Tikuisis P, Meunier P and Jubenville C 2001 Human body surface area: measurement and prediction using three dimensional body scans *European Journal of Applied Physiology* **85** 264-271

Tomita A, Miyamoto S and Horikoshi T 1999 Body surface area of Japanese young males and females *Japanese Journal of Biometrology* **36**(1) 43-51

Uusitupa T, Laakso I, Ilvonen S and Nikoskinen K 2010 SAR variation study from 300 to 5000 MHz for 15 voxel models including different postures *Phys. Med. Biol.* **55**(4) 1157-1176

Vouk V 1948 Projected Area of Convex Bodies *Nature*, **162** 330-331

Wang J, Suzuki T, Fujiwara O and Harima K 2012 Measurement and validation of GHz-band whole-body average SAR in a human volunteer using reverberation chamber *Phys. Med. Biol.* **57** 7893-7903